Role of AXL expression in non-small cell lung cancer

XIAOHAN QU[1], JINLU LIU[2], XINWEN ZHONG[1], XI LI[1] and QIGANG ZHANG[1]

[1]Department of Thoracic Surgery, The First Hospital of China Medical University, Shenyang, Liaoning 110001;
[2]Department of Ophthalmology, The Fourth Affiliated Hospital of China Medical University, Shenyang, Liaoning 110034, P.R. China

Received July 1, 2015; Accepted October 4, 2016

DOI: 10.3892/ol.2016.5356

Abstract. The present study aimed to investigate the expression profile of AXL in non-small cell lung cancer (NSCLC) and its clinical significance. The current study included 257 NSCLC patients, tyrosine-protein kinase receptor UFO (AXL) expression in paired lung cancer and adjacent normal lung tissues of NSCLC patients were compared by immunohistochemistry, western blot analysis and quantitative polymerase chain reaction (qPCR). These methods were used to detect the expression of the AXL gene and protein in fresh tissues from 35 patients. Small interfering RNA (siRNA) was transfected into the H1299 lung cancer cell line to knock down AXL expression; the effects of AXL-siRNA on cell proliferation and migration were examined by MTT and Transwell migration assay, respectively. It was found that AXL staining density in lung cancer tissues was significantly increased compared with adjacent normal lung tissues (55.25 vs. 26.85%; P<0.01); and the expression level of AXL in NSCLC patients was significantly associated with the degree of tumor differentiation (P<0.01) and the clinical stage of disease (P<0.01). Western blotting and qPCR showed that AXL expression was significantly higher in cancer tissues compared with that in adjacent lung tissue (P<0.05). Additionally, the current study also showed that AXL-siRNA inhibited H1299 cell proliferation and migration *in vitro*. The present study demonstrates the association between increased expression of AXL in NSCLC and the low differentiation phenotype, and its effects on cell proliferation and migration, suggesting its potential clinical values for the prognosis of NSCLC.

Introduction

Non-small cell lung cancer (NSCLC) is a lethal and aggressive malignancy that accounts for the majority of lung cancer cases. It is known to have low sensitivity to chemotherapy and even with optimal treatment, the mortality of NSCLC patients remains unacceptably high (1); therefore, the development of new treatment approaches for NSCLC is of great importance.

NSCLC has been shown to be induced by interplay between environmental factors and aberrant gene expression. However, a considerable amount of work has been performed to elucidate its genetic basis. The tyrosine-protein kinase receptor (TYRO3), tyrosine-protein kinase receptor UFO (AXL) and MER proto-oncogene tyrosine kinase (MER-TK) TAM receptor family, which share a common ligand termed growth arrest-specific 6 (Gas6), are characterized by a combination of 2 immunoglobulin-like domains, dual fibronectin type III repeats in the extracellular region and a cytoplasmic kinase domain. The activation of TAM signaling has been reported to be involved in several biological processes, including cell survival, proliferation, migration and adhesion (2). Belonging to the TAM subfamily, AXL, a receptor tyrosine kinase that shares the same structure and function with TYRO3 and MER, has been shown to be highly expressed in cancers including blood, breast, ovarian and prostate cancers (3-8). However, to the best of our knowledge, its potential role has not been fully addressed in NSCLC on a clinical level.

To fully understand its function in clinical patients, the present study enrolled a cohort of patients with NSCLC, of which the expression profile of AXL in cancer tissues and normal tissues were compared. A significant differential expression between tissues, and its association with clinical characteristics is reported. In addition to the clinical study, the *in vitro* experiments using AXL siRNA present consistency with the results of the present study.

Materials and methods

Patients and specimens. All samples used for paraffin-embedded sections were collected from the First Hospital of China Medical University (Shenyang, China) between January 2003 and December 2004, and consisted of a total number of 257 patients with surgically resected NSCLC and lung tissue adjacent to carcinoma tissues. All paracancerous lung tissues were at least 5 cm from the tumor edge. Frozen tissue samples (35 pairs) were obtained between July and December 2013 and kept in liquid nitrogen immediately following surgical resection and stored in a -70˚C refrigerator. None of the patients received any preoperative anticancer treatment. Relevant clinical data including gender, age, tumor size,

Correspondence to: Dr Qigang Zhang, Department of Thoracic Surgery, The First Hospital of China Medical University, 155 Nanjing North Street, Shenyang, Liaoning 110001, P.R. China
E-mail: lnqxh520@163.com

Key words: AXL, non-small cell lung cancer, expression

location, histological type, differentiation degree and lymph node metastasis were collected. The sampling procedures in all cases were reviewed and approved by the Ethics Committee of the Taizhou Hospital (Taizhou, China). The pathological diagnosis was confirmed by ≥2 experienced pathologists.

Immunohistochemistry analysis. Paraffin-embedded tissue sections were deparaffinized, rehydrated using xylene and a descending ethanol series, and washed with PBS. Antigen retrieval was performed by heating to 93˚C for 15 min. Following 30 min of endogenous peroxidase quenching and 30 min of blocking at 37˚C (both UltraSensitive™ SP kit; Maxim Biotech, Inc., Rockville, MD, USA), samples were incubated with the primary anti-AXL rabbit polyclonal antibody (1:100; cat. no. ab37861; Abcam, Cambridge, UK) overnight at 4˚C. Samples were subsequently washed with PBS and incubated with a biotin-labeled secondary antibody for 30 min at 37˚C, prior to incubation with streptavidin-peroxidase (both UltraSensitive™ SP kit) at 37˚C for 30 min, according to the manufacturer's protocol. 3,3-Diaminobenzidine (DAB) reagent (Maxvision™ DAB kit; Maxim Biotech, Inc.) was added for 45 sec to stain the samples. Images were captured using an inverted microscope (IX53; Olympus Corporation, Tokyo, Japan). The results were reported as the product of staining density score and staining intensity score. To determine the staining density score, which was defined as the percentage of the positive staining area, samples with a staining density <30% scored 1 point, samples with a staining density of between 30 and 60% scored 2 points, and samples with a staining density >60% scored 3 points. To determine the staining intensity score, samples with no color or yellowish color scored 1 point, samples with brown staining scored 2 points, and samples with dark brown staining scored 3 points. The results were determined by 2 experienced pathologists, and the mean of the three observations was taken to be the final score.

Cell culture. The 3 NSCLC cell lines used in the present study, adenocarcinoma A549, adenocarcinoma H1299 and squamous cell carcinomas SK-MES-1 were all obtained from the Cell Culture Center of the Forth Hospital of China Medical University (Shenyang, China). The H1299 cell line was cultured in RPMI-1640 medium (Hyclone: GE Healthcare Life Sciences, Logan, UT, USA), and the SK-MES-1 and A549 cell lines were cultured in Dulbecco's modified Eagle's medium (Hyclone: GE Healthcare Life Sciences). The media were supplied with 10% fetal bovine serum (Hyclone: GE Healthcare Life Sciences) without antibiotics. Cells were cultured in a 37˚C incubator containing 5% CO_2. The culture media were changed every 2-3 days. Cells with 80% confluency were passaged. Cells at 60-70% confluency were transfected with AXL-siRNA using Lipofectamine 2000 (Thermo Fisher Scientific, Inc., Waltham, MA, USA), Lipofectamine 2000 treatment alone was taken as the mock control. The target sequences were synthesized by Shanghai GenePharma Co., Ltd. (Shanghai, China) and are shown as follows: AXL-siRNA sense, 5'-GGAGACCCGUUA UGGAGAATT-3' and antisense, 5'-UUCUCCAUAACGGGU CUCCTT-3'; and negative control siRNA sense, 5'-GCGACG AUCUGCCUAAGAUdTdT-3' and antisense 5'-AUCUUA GGCAGAUCGUCGCdTdT-3'.

Western blot analysis. The protein from the fresh tissue was isolated and quantified using radioimmunoprecipitation assay buffer and a BCA Protein Assay kit (Beyotime Institute of Biotechnology, Haimen, China), respectively. The protein was denatured with loading buffer at 100˚C. The western blot analysis was conducted using a SDS-PAGE Gel kit (cat. no. P0012A) and the DAB Horseradish Peroxidase Color Development kit (cat. no. P0203) (both Beyotime Institute of Biotechnology) according to the manufacturer's protocol. The anti-AXL antibody was used at a dilution of 1:300. The mouse monoclonal antibodies against β-actin (cat. no. sc-47778; 1:500) were purchased from Santa Cruz Biotechnology, Inc. (Dallas, TX, USA). The results were analyzed using the Gel-Pro Analyzer software (version 4.0; Media Cybernetics, Inc., Rockville, MD, USA).

Reverse transcription-quantitative polymerase chain reaction (RT-qPCR). Quantitative analysis of AXL mRNA expression was achieved by RT-qPCR; the total RNA of the samples was isolated by RNAiso Plus (Takara Biotechnology Co., Ltd., Dalian, China), the first strand of cDNA was synthesized by PrimeScript® RT Master Mix Perfect Real Time (Takara Biotechnology Co., Ltd.), and the amplification was assessed using SYBR® Premix Ex Taq™ (Takara Biotechnology Co., Ltd.). All were completed according the manufacturer's protocols. Glyceraldehyde 3-phosphate dehydrogenase (GAPDH) was used as internal control. The relative expression was calculated by the $2^{-\Delta\Delta Cq}$ method. The primers were synthesized by Takara, and their sequences were as follows: AXL, forward, 5'-GCAACCTTCACCTACCGAGTTC-3' and reverse, 5'-GGC CAACATGGTGAAACCCT-3'; GAPDH, forward, 5'-ACCACA GTCCATGCCATCAC-3' and reverse 5'-TCCACCACCCTG TTGCTGTA-3'. The PCR amplification and data analysis were assessed using a ThermoCycler Dice Real Time System (Takara Biotechnology Co., Ltd.). The conditions were as follows: 1 cycle of 95˚C for 30 sec; 40 cycles of 95˚C for 5 sec and 60˚C for 30 sec; and 1 cycle 95˚C for 30 sec (Table I). Experiments were performed in triplicate and the mean ΔCq values were used for subsequent analysis.

Cell proliferation and invasion assays. Cells were plated into 24-well plates at a density of $3x10^4$ cells/well 1 day prior to transfection. Cell culture medium was replaced with fresh RPMI-1640 medium containing 10% fetal bovine serum without antibiotics one day following AXL-siRNA transfection. Following another 24, 48 and 72 h of culture, the MTT Cell Proliferation Assay kit (American Type Culture Collection, Manassas, VA, USA) was used to perform the MTT assay, according to the manufacturer's protocol. Each group was detected at a wavelength of 490 nm using a Model 680 Microplate Reader (Bio-Rad, Hercules, CA, USA). Experiments were performed in triplicate and the mean was used in the statistical analysis. The Transwell invasion assay was performed using a 24-well, 8 μm pore size Costar Transwell chamber system (Corning Life Sciences, Lowell, MA, USA), according to the manufacturer's protocol. A total of $1x10^5$ cells/well were seeded in the upper chamber. The number of cells in the lower chamber was counted in the lower chamber following 36 h of culture for the transfection and control groups. Experiments were performed in triplicate and the mean was used in the statistical analysis.

Table I. Reverse transcription quantitative PCR reaction conditions.

Condition	Initial denaturation	Amplification stage		Melt curve
Cycle number	1	40		1
Temperature, ˚C	95	95	60	95
Time, sec	30	5	30	30

PCR, polymerase chain reaction.

Table II. Expression of AXL in tumor and peritumoral tissues.

		Expression of AXL			
Tissue	n	-	+	Positive rate	P-value
Tumor	257	115	142	55.25%	0.009[a]
Peritumoral	257	188	69	26.85%	

[a]P-value relates to comparison of positive rate between tumor and peritumoral tissue. AXL, tyrosine-protein kinase receptor UFO.

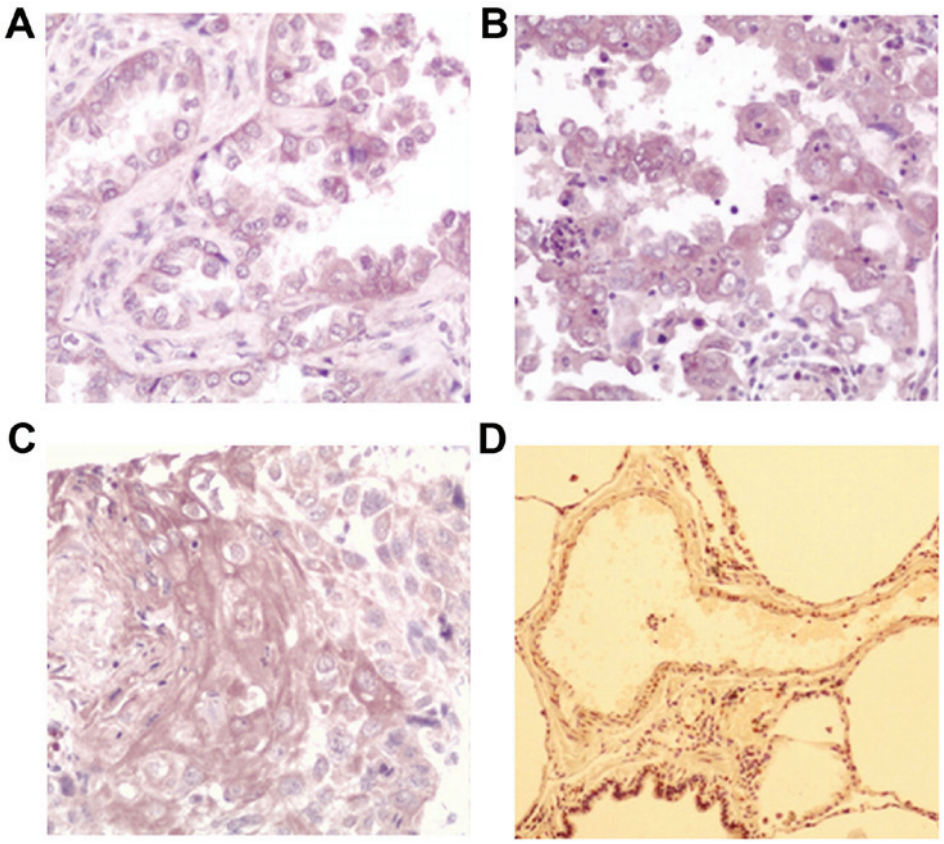

Figure 1. Expression of AXL in NSCLC tissue and the adjacent lung tissue. (A) Well-differentiated adenocarcinoma (magnification, x200), (B) Poorly-differentiated adenocarcinoma (magnification, x200), (C) Well-differentiated squamous cell carcinoma (magnification, x200), (D) adjacent normal lung tissue (magnification, x40). AXL, tyrosine-protein kinase receptor UFO; NSCLC, non-small cell lung cancer.

Statistical analysis. The data were analyzed by SPSS 19.0 software (IBM SPSS, Armonk, NY, USA); the means between two groups were compared by paired *t*-test and Mann-Whitney U test, and the analysis of the associations between AXL expression and clinical characteristics was assessed by χ^2 test or Fisher's exact test. A two tailed $P<0.05$ was considered to indicate a statistically significant difference.

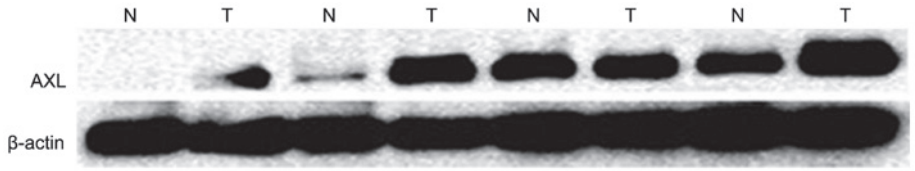

Figure 2. Protein level of AXL in fresh non-small cell lung cancer tissues and adjacent lung tissues as determined by western blot analysis. T, tumor; N, peritumoral; AXL, tyrosine-protein kinase receptor UFO.

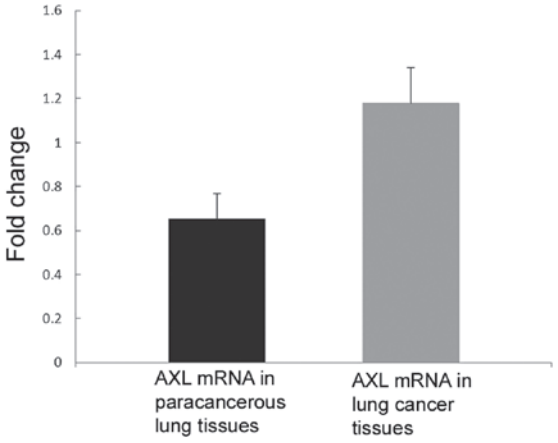

Figure 3. mRNA level of AXL in fresh NSCLC tissues and adjacent lung tissues from 35 patients as determined by quantitative polymerase chain reaction. The mRNA levels of AXL were significantly increased in NSCLC tissues compared with those in adjacent lung tissues (P=0.037). AXL, tyrosine-protein kinase receptor UFO.

Results

Differential expression of AXL in NSCLC tissue and its clinical significance. The results of the immunohistochemistry analysis are shown in Fig. 1. The present study found that the AXL staining was mainly located in the cytoplasm, and a small portion of nuclear staining was also observed. Out of the total 257 patients 147 showed positive staining for AXL, and the average positive rate was 55.25%, which is significantly higher than that of the adjacent lung tissue (26.85%; P=0.009; Table II).

The clinical characteristics and the statistical analysis are shown in Table III. The present study found that the expression level of AXL was significantly associated with the degree of tumor differentiation. The lower the differentiation of the tumor, the higher level of AXL expressed (P=0.001). Patients with a stage higher than stage I showed significantly higher expression level of AXL than those with stage I (P=0.005). By contrast, no association between AXL expression and age (P=0.722), gender (P=0.238), histological type (P=1.000), lymph node metastasis (P=0.091) or tumor size (P=0.166) was found.

Next, the expression of AXL in fresh tissues was detected by western blot analysis and qPCR. Consistent with the immunohistochemistry results, the mRNA (P=0.037; Fig. 3) and protein (P=0.044; Fig. 2) levels of AXL were significantly increased in NSCLC tissues compared with those in their adjacent lung tissues.

Differential expression of AXL in NSCLC cell lines. To investigate the function of AXL *in vitro*, the current study first detected its expression in lung cancer cell lines A549, H1299 and SK-MES-1 by western blot analysis and qPCR. As shown in Fig. 4, H1299 demonstrated markedly higher level of AXL protein expression compared with the other two cell lines. In

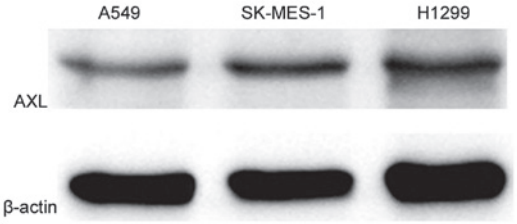

Figure 4. Protein level of AXL in non-small cell lung cancer cell lines as determined by western blot analysis. H1299 cells exhibited markedly increased AXL protein expression compared with the other two cell lines. AXL, tyrosine-protein kinase receptor UFO.

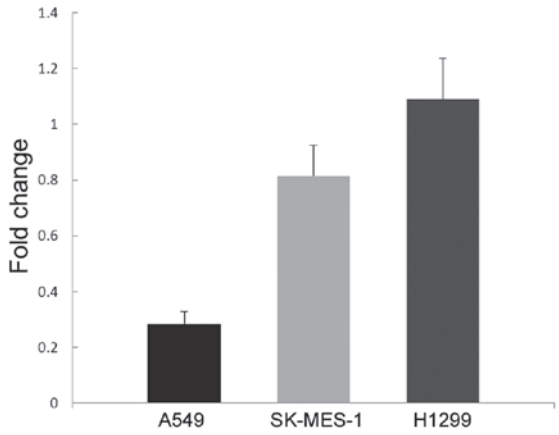

Figure 5. mRNA level of AXL in non-small cell lung cancer cell lines as determined by quantitative polymerase chain reaction. H1299 cells exhibited significantly increased AXL expression compared with the other two cell lines at the mRNA level (P=0.003 vs. A549 cells; P=0.005 vs. SK-MES-1 cells). AXL, tyrosine-protein kinase receptor UFO.

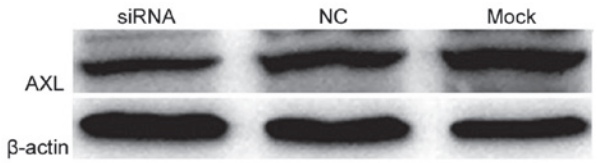

Figure 6. Effect of AXL-siRNA on the protein level of AXL, as determined by western blot analysis. AXL protein expression was markedly decreased following siRNA-mediated knockdown of AXL compared with the negative control and mock-transfected cells. AXL, tyrosine-protein kinase receptor UFO; siRNA, small interfering RNA; NC, negative control.

Table III. Associations between the expression of AXL and the clinical characteristics.

Variable	Patients, n	Expression of AXL, n -	+	Positive rate, %	P-value[a]
Total	257				
Gender					0.238
Male	190	81	109	57.37	
Female	67	36	31	46.27	
Age					0.722
≤60 years	111	48	63	56.76	
>60 years	146	69	77	52.74	
Histological type					1.000
Adenocarcinoma	143	66	77	53.85	
Squamous cell carcinoma	114	51	63	55.26	
Differentiation					0.001
Well	44	33	11	25.00	
Moderate	140	71	69	49.29	
Poor	73	13	60	82.19	
TNM stage					0.005
Stage I	47	35	12	25.53	
>Stage I	210	83	127	60.48	
Lymph node metastasis					0.091
Yes	115	44	71	61.74	
No	142	73	69	48.59	
Tumor size					0.166
≤3 cm	92	50	42	45.65	
>3 cm	165	67	98	59.39	

[a]P-values relate to comparison of positive rate between tumor and peritumoral tissue. AXL, tyrosine-protein kinase receptor UFO; TNM, TNM classification of malignant tumors.

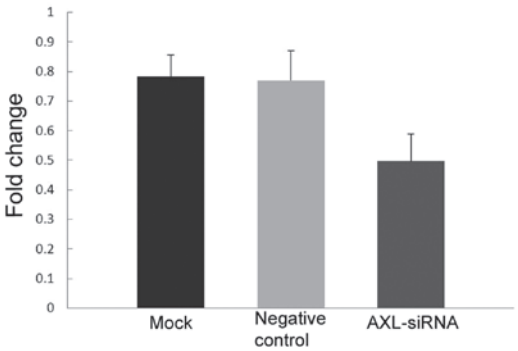

Figure 7. Effect of AXL-siRNA on the mRNA level of AXL as determined by quantitative polymerase chain reaction. mRNA levels were significantly decreased following siRNA-mediated knockdown of AXL compared with the negative control (P=0.019) and mock-transfected (P=0.013) cells. AXL, tyrosine-protein kinase receptor UFO; siRNA, small interfering RNA.

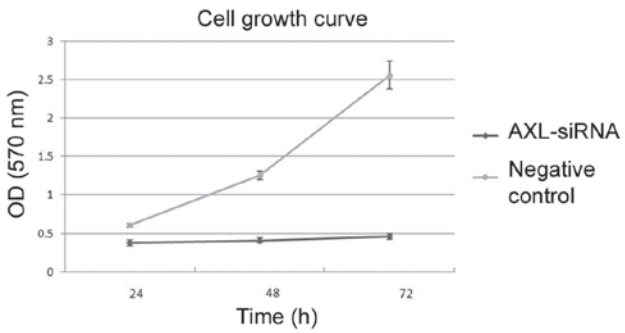

Figure 8. The effect of AXL-siRNA on cell proliferation as determined by methyl thiazolyl tetrazolium assay (P=0.007 vs. the negative control). AXL, tyrosine-protein kinase receptor UFO; siRNA, small interfering RNA; OD, optical density.

addition, H1299 cells demonstrated significantly increased AXL mRNA expression (P=0.003 vs. A549 cells; P=0.005 vs. SK-MES-1 cells; Fig. 5).

Effects of AXL-siRNA on the proliferation and invasion activity of H1299 cells. Due to the relative high expression of H1299, a methyl thiazolyl tetrazolium (MTT) assay was performed with a Transwell migration assay to determine whether inhibition of AXL expression could reduce its

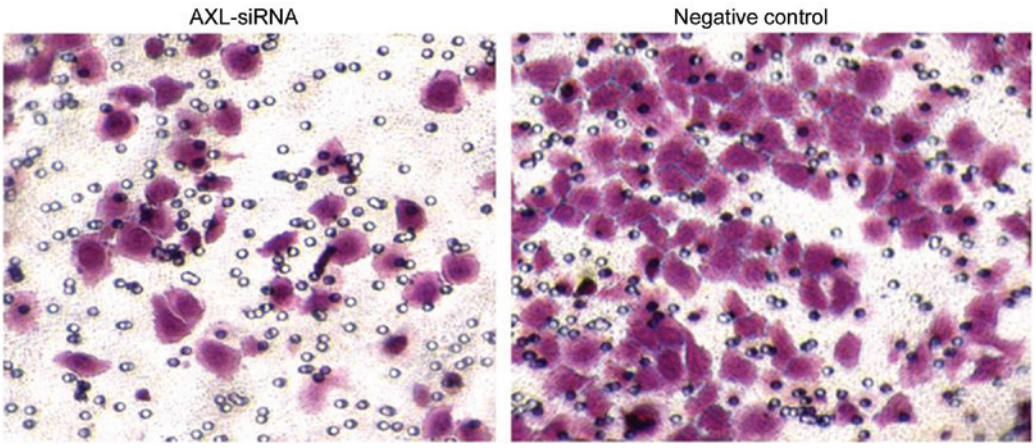

Figure 9. AXL depletion inhibits cell invasion *in vitro*. Representative photomicrographs of Transwell results for H1299 cells (magnification, x200). AXL, tyrosine-protein kinase receptor UFO; siRNA, small interfering RNA.

proliferation and invasion activity. Western blotting and qPCR analysis confirmed the knockdown efficiency of the AXL-siRNA. AXL protein expression was markedly decreased (Fig. 6) and AXL mRNA expression was significantly decreased (P=0.019 vs. the negative control; P=0.013 vs. the mock transfection; Fig. 7) in H1299 cells following the silencing of AXL by its specific siRNA.

Subsequent to transfection, cells were incubated in complete medium for another 24, 48 or 72 h. MTT results showed that transfection with AXL-siRNA resulted in a significant decrease of cell viability compared with the negative control at each time point (P=0.007; Fig. 8). In addition, the number of cells in the bottom layer of the culture was significantly decreased following AXL-siRNA transfection compared with the negative control (P=0.018). The number of cells that migrated to the underside of the membranes was calculated by counting 5 random separate fields, as shown by Transwell analysis (Fig. 9), indicating the decreased invasion activity subsequent to AXL inhibition.

Discussion

In the present study, the expression of AXL was detected in the paraffin sections of NSCLC tissues. Consistent with the feature of receptor tyrosine kinases, it was found that the expression of AXL was largely localized in the cytoplasm, with the exception of a small proportion of nuclear localization. More importantly, the expression of AXL was found to be significantly higher in tumor tissues compared with adjacent lung tissues in the two paraffin sections and fresh tissues, which is in accordance with the findings of a previous study (9). Subsequent to reviewing the clinical characteristics statistically, the present study found a significant association between high AXL expression and low differentiation grade. As atypical histopathology forms an important part of the low differentiation state, the current study suggests that the higher AXL expression may be associated to an atypical phenotype of NSCLC cells, thus represents a cancer type with aggressive invasion and poor prognosis. Similarly, the present data also revealed a strong association between high AXL expression and tumor Union for International Cancer Control TNM Classification of Malignant Tumors stage (10), patients with a disease stage >I showed an overall higher AXL expression compared with stage I patients. The current clinical data therefore preliminarily demonstrated that AXL may be a risk factor associated with the prognosis of NSCLC patients.

Demarchi *et al* demonstrated the anti-apoptotic function of AXL by activating the nuclear factor κB (NF-κB) pathway in NIH3T3 fibroblast cells (11). Shankar *et al* reported the synergic effect of Gas6 on AXL in the regulation of apoptosis, and found that Gas6 promoted cell survival and decreased apoptosis in AXL-expressing oligodendrocytes in the presence of growth factor deprivation and tumor necrosis factor-cytotoxicity (12). In addition to these findings, Gas6/AXL activation has been shown to be involved in the processes of proliferation and apoptosis of human pulmonary artery endothelial cells, human umbilical vein smooth muscle cells and human umbilical vein endothelial cells by several mechanisms including protein kinase B activation, NF-κB phosphorylation, B-cell lymphoma 2 upregulation and caspase-3 suppression (13-15).

A number of studies have also highlighted the significant role of AXL in lung cancer cell invasion and metastasis. Tai *et al* (16) suggested that NF-kB dependent matrix metalloproteinase-9 activation mediates the pro-metastatic effect of AXL on lung cancer cells. Particularly, by co-immunoprecipitation and RNAi methods, Vaughan *et al* (17) demonstrated that mutated p53 is responsible for increased AXL expression, and that increased expression may have accounted for the enhancement of mitogenic activity. In the present study, since the AXL expression was significantly increased in H1299 cells compared with other NSCLC cell lines, the effect of AXL knockdown on H1299 cell proliferation and migration was investigated. The current data indicated the detrimental effect of AXL on cancer cells, as exemplified by the decreased proliferation and migration capacity subsequent to knockdown of AXL.

In summary, the present study reported aberrantly higher expression of AXL in NSCLC tissues, and this expression profile is prominently associated with the histological grade and clinical stage, which offered insights into its potential prognostic value. Previous studies have shed new light on AXL-based targeted therapy; however, additional elucidations

on the molecular regulatory network of AXL in the development and progression of lung cancer are required to facilitate its application in translational medical research.

References

1. Jemal A, Bray F, Center MM, Ferlay J, Ward E and Forman D: Global cancer statistics. CA Cancer J Clin 61: 69-90, 2011.
2. Verma A, Warner SL, Vankayalapati H, Bearss DJ and Sharma S: Targeting Axl and Mer kinases in cancer. Mol Cancer Ther 10: 1763-1773, 2011.
3. Li Y, Ye X, Tan C, Hongo JA, Zha J, Liu J, Kallop D, Ludlam MJ and Pei L: Axl as a potential therapeutic target in cancer: Role of Axl in tumor growth, metastasis and angiogenesis. Oncogene 28: 3442-3455, 2009.
4. Hong CC, Lay JD, Huang JS, Cheng AL, Tang JL, Lin MT, Lai GM and Chuang SE: Receptor tyrosine kinase AXL is induced by chemotherapy drugs and overexpression of AXL confers drug resistance in acute myeloid leukemia. Cancer Lett 268: 314-324, 2008.
5. Liu L, Greger J, Shi H, Liu Y, Greshock J, Annan R, Halsey W, Sathe GM, Martin AM and Gilmer TM: Novel mechanism of lapatinib resistance in HER2-positive breast tumor cells: Activation of AXL. Cancer Res 69: 6871-6878, 2009.
6. Dunne PD, McArt DG, Blayney JK, Kalimutho M, Greer S, Wang T, Srivastava S, Ong CW, Arthur K, Loughrey M, *et al*: AXL is a key regulator of inherent and chemotherapy-induced invasion and predicts a poor clinical outcome in early-stage colon cancer. Clin Cancer Res 20: 164-175, 2014.
7. Rankin EB, Fuh KC, Taylor TE, Krieg AJ, Musser M, Yuan J, Wei K, Kuo CJ, Longacre TA and Giaccia AJ: AXL is an essential factor and therapeutic target for metastatic ovarian cancer. Cancer Res 70: 7570-7579, 2010.
8. Sainaghi PP, Castello L, Bergamasco L, Galletti M, Bellosta P and Avanzi GC: Gas6 induces proliferation in prostate carcinoma cell lines expressing the Axl receptor. J Cell Physiol 204: 36-44, 2005.
9. Shieh YS, Lai CY, Kao YR, Shiah SG, Chu YW, Lee HS and Wu CW: Expression of axl in lung adenocarcinoma and correlation with tumor progression. Neoplasia 7: 1058-1064, 2005.
10. Sobin LH and Compton CC: TNM seventh edition: What's new, what's changed: Communication from the international union against cancer and the American Joint Committee on cancer. Cancer 116: 5336-5339, 2010.
11. Demarchi F, Verardo R, Varnum B, Brancolini C and Schneider C: Gas6 anti-apoptotic signaling requires NF-kappa B activation. J Biol Chem 276: 31738-31744, 2001.
12. Shankar SL, O'Guin K, Kim M, Varnum B, Lemke G, Brosnan CF and Shafit-Zagardo B: Gas6/Axl signaling activates the phosphatidylinositol 3-kinase/Akt1 survival pathway to protect oligodendrocytes from tumor necrosis factor alpha-induced apoptosis. J Neurosci 26: 5638-5648, 2006.
13. Melaragno MG, Cavet ME, Yan C, Tai LK, Jin ZG, Haendeler J and Berk BC: Gas6 inhibits apoptosis in vascular smooth muscle: Role of Axl kinase and Akt. J Mol Cell Cardiol 37: 881-887, 2004.
14. Lee WP, Wen Y, Varnum B and Hung MC: Akt is required for Axl-Gas6 signaling to protect cells from E1A-mediated apoptosis. Oncogene 21: 329-336, 2002.
15. Hasanbasic I, Cuerquis J, Varnum B and Blostein MD: Intracellular signaling pathways involved in Gas6-Axl-mediated survival of endothelial cells. Am J Physiol Heart Circ Physiol 287: H1207-H1213, 2004.
16. Tai KY, Shieh YS, Lee CS, Shiah SG and Wu CW: Axl promotes cell invasion by inducing MMP-9 activity through activation of NF-kappaB and Brg-1. Oncogene 27: 4044-4055, 2008.
17. Vaughan CA, Singh S, Windle B, Yeudall WA, Frum R, Grossman SR, Deb SP and Deb S: Gain-of-function activity of mutant p53 in lung cancer through Up-regulation of receptor protein tyrosine kinase Axl. Genes Cancer 3: 491-502, 2012.